Fluorescence Studies of Ligand-Induced Conformational Changes of the Na^+/Glucose Cotransporter†

Anne-Kristine Meinild, Bruce A. Hirayama, Ernest M. Wright, and Donald D. F. Loo*

Department of Physiology, UCLA School of Medicine, Center for the Health Sciences, Los Angeles, California 90095-1751

Received August 14, 2001; Revised Manuscript Received November 15, 2001

ABSTRACT: Conformational changes in the human Na^+/glucose cotransporter (hSGLT1) were examined using hSGLT1 Q457C expressed in *Xenopus laevis* oocytes and tagged with tetramethylrhodamine-6-maleimide (TMR6M). Na^+/glucose cotransport is abolished in the TMR6M-labeled mutant, but the protein binds Na^+ and sugar [Loo et al. (1998) *Proc. Natl. Acad. Sci. U.S.A. 95*, 7789−7794]. Under voltage clamp the fluorescence of labeled Q457C was dependent on external cations. Increasing [Na^+] increased fluorescence with a Hill coefficient of 2 and half-maximal concentration ($K_{0.5}^{Na}$) of 49 mM at −90 mV. Li^+ also increased fluorescence, whereas choline, tetraethylammonium, and *N*-methyl-D-glucamine did not. Fluorescence was increased by sugars with specificity: methyl α-D-glucopyranoside > D-glucose > D-galactose ≫ D-mannitol. Voltage-jump experiments (in 100 mM NaCl buffer in absence of sugar) elicited parallel changes in pre-steady-state charge movement and fluorescence. Charge vs voltage and fluorescence vs voltage curves followed Boltzmann relations with the same median voltage ($V_{0.5} = -50$ mV), but the apparent valence was 1 for charge movement and 0.4 for fluorescence. $V_{0.5}$ for fluorescence and charge movement was shifted by −100 mV per 10-fold decrease in [Na^+]. Under Na^+-free conditions, there was a voltage-dependent change in fluorescence. Voltage-jump experiments showed that the maximal change in fluorescence increased 20% with sugar. These results indicate that Na^+, sugar, and membrane voltage change the local environment of the fluorophore at Q457C. Our interpretation of these results is (1) the conformational change of the empty transporter is voltage dependent, (2) two Na^+ ions can bind cooperatively to the protein before sugar, and (3) sugar binding induces a conformational change.

The Na^+/glucose cotransporter (SGLT1)[1] is a member of a large class of membrane proteins that couples the electrochemical potential gradient for Na^+ to the uphill transport of substrates (sugars, vitamins, and ions). It is now well established that two Na^+ ions are transported with each sugar molecule and that protein conformational changes are involved in the coupling of Na^+ and sugar transport (*1*, *2*). However, the order of substrate binding to the transporter and the conformational changes of the transporter induced by substrates are not as well understood. We have strong evidence that two Na^+ ions bind to the transporter before glucose and that Na^+/glucose cotransport occurs via a series of conformational changes induced by ligands (*2*, *3*). In the absence of sugar, SGLT1 exhibits a pre-steady-state current (or charge movement) with step changes in membrane voltage; we attributed the charge movement to conformational changes of the transporter (*2*, *4*−*6*).

It has previously been shown that the human SGLT1 mutant protein Q457C is a fully functional Na^+/glucose cotransporter. Residue 457 is located at the interface between transmembrane segment (TMS) 11 and the extracellular fluid. TMS 11 is one of five C-terminal helices (TMS 10−14) thought to form the sugar pathway (*7*, *8*). After exposure to many thiol-reactive reagents (such as methanethiosulfonates and maleimides) sugar transport is abolished, but the protein retains its ability to bind Na^+ and sugar (*2*). Accessibility of Q457C to thiol-reactive reagents depended on membrane voltage and Na^+ concentrations and was dependent on the conformations of the transporter. There was a direct relationship between accessibility of Q457C to thio-reactive reagents and the pre-steady-state charge movement of SGLT1, thus suggesting that the charge movement is due to conformational changes of the transporter in response to changes in membrane voltage (*2*). Simultaneous voltage-jump and fluorescence experiments with the tetramethylrhodamine-6-maleimide- (TMR6M-) labeled human SGLT1 Q457C showed a change in the rhodamine fluorescence concurrent with the pre-steady-state charge movement (*2*).

In this study, we examine the ligand and voltage-induced changes in SGLT1 conformation by monitoring the fluorescence of TMR6M-labeled human SGLT1 Q457C expressed in *Xenopus laevis* oocytes. Since sugar transport is abolished,

† This research was supported by NIH Grants DK19567, DK44602, and GM52094 and by a postdoctoral fellowship from the Carlsberg Foundation (to A.-K.M).

* To whom correspondence should be addressed. Phone: 310-206-8569. Fax: 310-208-5881. E-mail: dloo@mednet.ucla.edu.

[1] Abbreviations: SGLT1, Na^+/glucose cotransporter; hSGLT1, human Na^+/glucose cotransporter; TMR6M, tetramethylrhodamine-6-maleimide; ΔF, change in fluorescence intensity; DC fluorescence, background steady-state fluorescence; ΔF_{max}, maximal fluorescence change; $V_{0.5}$, membrane potential at 50% ΔF_{max}; *z*, apparent valence of the movable charge; *Q*, pre-steady-state charge movement; αMDG, methyl α-D-glucopyranoside; D-Glu, D-glucose; D-Gal, D-galactose; TEA^+, tetraethylammonium; $NMDG^+$, *N*-methyl-D-glucamine; TMS, transmembrane segment; $K_{0.5}$, half-maximal substrate concentration; τ, relaxation time constant; au, arbitrary unit of fluorescence intensity; V_m, test potential; V_h, holding potential.

10.1021/bi011661r CCC: $22.00
Published on Web 12/29/2001

the partial reactions involved in sugar transport are eliminated, and this allows us to examine the conformational changes involved in Na^+ and sugar binding. Our results indicate that there is a voltage-dependent change in the conformation of the empty transporter. Two Na^+ ions can bind to the transporter before sugar, and sugar binding induces another conformational change of the transporter.

MATERIALS AND METHODS

Preparation and Maintenance of Oocytes. Mature *X. laevis* oocytes were isolated, defolliculated, injected with 50 ng of human SGLT1 Q457C cRNA, and maintained at 18 °C in Barth's medium containing 1 mg/mL gentamicin/streptomycin for 3−7 days prior to experiments as previously described (*2*).

hSGLT1 Q457C was labeled (≥90%) with 200 μM tetramethylrhodamine-6-maleimide (TRM6M, purchased from Molecular Probes) in NaCl buffer (100 mM NaCl, 2 mM KCl, 1 mM $MgCl_2$, 1 mM $CaCl_2$, 10 mM HEPES, pH 7.4) for 5 min at 20−23 °C with the membrane potential (V_m) clamped at −90 mV in the dark (*2*). After labeling, the oocytes were transferred to NaCl buffer free of dye and kept in the dark until use.

Combined Voltage-Clamp and Fluorescence Experiments. Electrophysiological and fluorescence experiments were performed simultaneously. The membrane potential was controlled and the currents were measured using the two-electrode voltage clamp (*2*). Fluorescence was measured using a Hamamatsu S5590 silicon photodiode (Hamamatsu City, Japan) connected to the camera port of an Olympus BX50WI epifluorescence microscope (Olympus America Inc., Melville, NY). We have found that the DC, or steady-state, fluorescence was lowest and the fluorescence signal more stable when the animal pole faced the fluorescence objective; thus in all experiments the oocytes were placed in this orientation. The oocyte membrane was illuminated with a 150 W tungsten lamp and excitation and emission filters at 535 and 580 nm (Olympus filter set U-M576). An electronic shutter (Uniblitz VS25S2T1, Vincent Associates, Rochester, NY), synchronized with the voltage pulse, was placed between the lamp and the preparation to minimize photobleaching. The experiments were controlled using the program Clampex of pClamp7 (Axon Instruments, Union City, CA). The pre-steady-state current and the fluorescence signal were simultaneously measured. The fluorescent signal was amplified 100×, low-pass filtered at 1 kHz using an eight-pole Bessel filter (LPF-8, Warner Instrument Corp., Hamden, CT), and digitized at 200 μs per point. Fluorescence intensity is expressed as arbitrary units (au).

All experiments were performed under continuous perfusion of the bath solution. Two types of experiments were performed: (1) concentration "jumps" where the composition of the external solution was changed (with a half-time $t_{1/2}$ of 3−5 s) while membrane potential was maintained constant, and (2) voltage jumps in which membrane voltage was stepped for 75 ms from the holding (V_h) to a series of test voltages (V_m). In the concentration-jump experiments, the fluorescence was measured every 2 s by opening of the shutter for 80 ms. Experiments were performed at room temperature (20−23 °C). Na^+-free solutions were prepared by substituting choline chloride, tetraethylammonium (TEA^+) chloride, *N*-methyl-D-glucamine (NMDG) chloride, or RbCl for NaCl. The steady-state substrate- (sugar-) induced currents were measured (at each membrane voltage) as the difference in current before and after addition of sugar [100 mM methyl α-D-glucopyranoside (αMDG), a nonmetabolizable glucose analogue] to the bath solution.

Rundown of Fluorescence. In the course of an experiment, there was a rundown of both the steady-state and the voltage-dependent fluorescent signals due to "washout" of noncovalently bound fluorophore and photobleaching. Photobleaching was minimized by using an electronic shutter as described above. The rate of rundown of fluorescence depended on the darkness of the animal pole. In oocytes with black animal poles, total fluorescence intensity was reduced by ∼20% with a $t_{1/2}$ of 30 min. Rundown of the fluorescence signal followed an approximate exponential time course and was compensated for by comparing the control values at the beginning and end of each test run. All of the data have been corrected for rundown.

Data Analysis. There was a pre-steady-state transient current (charge movement) associated with SGLT1 with step jumps in membrane voltage (*2*, *4*−*6*). The pre-steady-state current was obtained by fitting the total oocyte membrane current (I) to the equation:

$$I(t) = I_1 \exp(-t/\tau_1) + I_2 \exp(-t/\tau_2) + I_{ss}$$

where t is time, $I_1 \exp(-t/\tau_1)$ is the oocyte membrane capacitive transient with initial value I_1 and time constant τ_1, $I_2 \exp(-t/\tau_2)$ is the pre-steady-state current of Q457C with initial value I_2 and time constant τ_2, and I_{ss} is the steady-state current. Q457C pre-steady-state current was obtained from the total current by subtraction of the capacitive and steady-state components (*2*, *5*). At each membrane voltage, the pre-steady-state charge movement (Q) was obtained from the time integral of the pre-steady-state current (*5*).

The dependence of the change of fluorescence intensity (ΔF) on external substrates was fitted to the equation:

$$\Delta F = (\Delta F_{max}[S]^n)/\{[S]^n + (K_{0.5})^n\} \quad (1)$$

where [S] is the external substrate (Na^+ or sugar) concentration, ΔF_{max} is the maximal change in fluorescence intensity for saturating [S], $K_{0.5}$ is the half-maximal substrate concentration, and n is the Hill coefficient.

The Boltzmann equation was used to fit the dependence of change of fluorescence intensity (ΔF) on membrane voltage. ΔF vs V relations were fitted to the Boltzmann function:

$$(\Delta F - \Delta F_{hyp})/\Delta F_{max} = 1/[1+\exp(z(V_m - V_{0.5})F/RT)] \quad (2)$$

where $\Delta F_{max} = \Delta F_{dep} - \Delta F_{hyp}$, ΔF_{dep} and ΔF_{hyp} are the ΔF at depolarizing and hyperpolarizing limits, F is the Faraday, R is the gas constant, T is the absolute temperature, $V_{0.5}$ is the membrane potential at 50% ΔF_{max}, and z is apparent valence of the charge sensor of the fluorophore. The Boltzmann relation was also used to fit the dependence of pre-steady-state charge movement (Q) on membrane voltage (*2*, *5*). The parameters obtained were the maximal charge (Q_{max}), the membrane voltage at 50% Q_{max} ($V_{0.5}$), and apparent valence of the movable charge (z).

Fits of data to equations were performed using Sigmaplot 2000 (SPSS, Chicago, IL). Unless otherwise noted, statistics

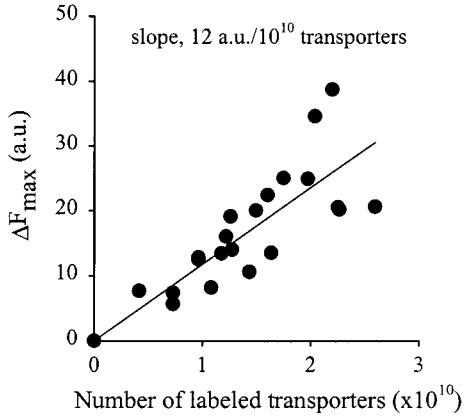

FIGURE 1: Correlation between rhodamine fluorescence (ΔF_{max}) and number of labeled human SGLT1 Q457C. The expression level of hSGLT1 Q457C in the oocyte plasma membrane was measured as the sugar-dependent current induced by the addition of 100 mM αMDG to the NaCl buffer at $V_m = -150$ mV. The oocytes were then labeled with TMR6M under voltage clamp conditions at −90 mV in the NaCl buffer as described in Materials and Methods. After labeling, the sugar-dependent current was again measured. The number of labeled Q457C transporters was determined from the ratio $\Delta I_{sug}/r$, where ΔI_{sug} is the difference in the sugar-evoked current before and after labeling and r is the turnover number of hSGLT1 Q457C. r was estimated from the ratio (I_{max}/Q_{max}; *5*) of the steady-state current (I_{max}) induced by saturating sugar concentrations and the maximal pre-steady-state charge movement (Q_{max}). For hSGLT1 Q457C, r was 58 ± 4 s^{-1} ($n = 3$) at $V_m = -150$ mV. The membrane voltage was held at −50 mV and then jumped to +50 and −150 mV. The difference in steady-state rhodamine fluorescence between +50 and −150 mV, denoted by ΔF_{max} (expressed in arbitrary units, au), is plotted against the number of labeled hSGLT1 Q457C transporters. The slope of the regression line is 12 ± 1 au/10^{10} transporters.

expressed were obtained from the error of the fit. While data are shown for representative experiments, all experiments were performed on at least three oocytes from different batches.

RESULTS

Correlation between Fluorescence and the Number of Human SGLT1 Q457C Transporters Labeled by Rhodamine. There was a direct correlation between the maximal change in fluorescence (ΔF_{max}) of TMR6M-labeled Q457C and the number of rhodamine-labeled hSGLT1 Q457C cotransporters (Figure 1). The number of labeled cotransporters was estimated from the ratio of the loss of sugar-evoked current after labeling and the turnover number of Q457C (58 s^{-1}; see figure legend). The sugar current lost by labeling was obtained by subtracting the residual sugar-evoked current after labeling from the sugar-evoked current before labeling at $V_m = -150$ mV with 100 mM αMDG. The slope of the regression line was 12 ± 1 au/10^{10} transporters.

In contrast to the voltage-dependent fluorescence signal, the background or DC fluorescence (in the range 200−700 au and measured at $V_m = -50$ mV in the 100 mM NaCl buffer) was variable among the labeled oocytes. The major determinant of DC fluorescence was the color of the animal pole: oocytes with black animal poles exhibited the lowest DC fluorescence. $\Delta F_{max}/F$, the ratio of the maximal change in fluorescence (between +90 and −190 mV) to DC fluorescence varied between 1.9% and 8.4%, with a mean of $4.7 \pm 0.4\%$ ($n = 21$).

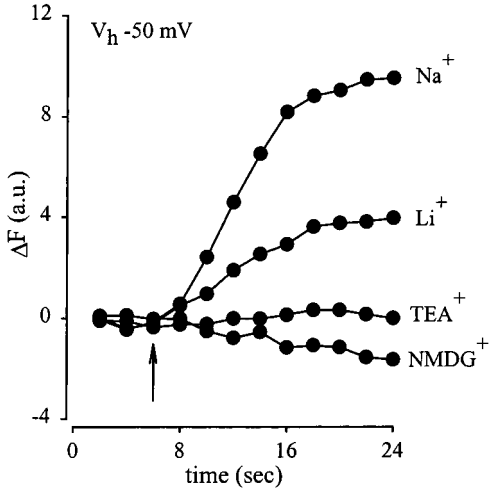

FIGURE 2: Cation dependence of fluorescence. Time course of the fluorescence on an oocyte expressing Q457C labeled with TMR6M. External perfusing solution initially contained 0 Na^+ (100 mM choline chloride), and membrane potential was held at −50 mV. At the arrow, the perfusing solution was changed from choline buffer to either 100 mM Na^+, Li^+ TEA^+, or $NMDG^+$.

We compared the DC fluorescence of TMR6M-labeled noninjected oocytes and oocytes expressing wild-type human SGLT1 [expression level was 790 ± 69 nA ($n = 5$) at −150 mV with 10 mM αMDG]. The DC fluorescence level for the controls was 187 ± 15 au ($n = 5$) and for oocytes expressing human SGLT1 was 160 ± 10 au ($n = 4$). On the same batch of oocytes, the DC fluorescence for TMR6M-labeled hSGLT1 Q457C expressing oocytes was 229 ± 25 au ($n = 3$). The nonsignificant difference between the control oocytes and oocytes expressing wild-type human SGLT1 indicates that the endogenous cysteines in human SGLT1 are not labeled by TMR6M. In addition, exposing oocytes expressing wild-type human SGLT1 to TMR6M under the same labeling conditions as for Q457C had no effect on the αMDG-induced currents. Finally, no change of fluorescence was observed on varying Na^+ and sugar concentrations and membrane voltage in either control oocytes or oocytes expressing wild-type human SGLT1 (data not shown).

Cation Specificity. The rhodamine fluorescence of hSGLT1 Q457C was dependent on the cations in the external medium. This is illustrated in Figure 2 for an experiment where the membrane potential was held at −50 mV, and the oocyte was superfused with a buffer free of Na^+ (100 mM choline chloride buffer). At the time marked by the arrow, the superfusing buffer was replaced by different solutions where choline was substituted for Na^+, Li^+, TEA^+, or $NMDG^+$. Upon replacement of choline by Na^+ the fluorescence intensity increased (from the baseline) to a steady-state level with a half-time ($t_{1/2}$) of 3−5 s (time required for changing bath solution). When Li^+ replaced choline, the fluorescence also increased (40%). The increases in the fluorescence intensity observed in Na^+ and Li^+ were reversible: when the bath solution was returned to choline buffer, the fluorescence returned to the baseline level. When choline was replaced by TEA^+, $NMDG^+$, and Rb^+ (not shown), there was no effect on fluorescence.

Na^+ Dependence. Figure 3 shows an experiment where the fluorescence increase (ΔF) was measured as [Na^+] was varied from 0 to 100 mM and the membrane potential was

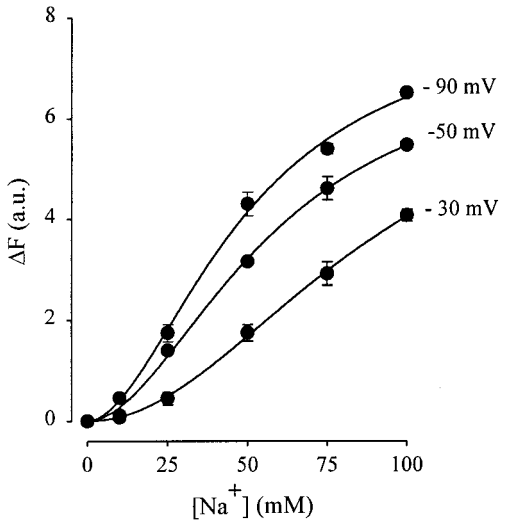

FIGURE 3: Na^+ dependence of fluorescence. The kinetics of Na^+ activation was determined by measuring the increase in fluorescence (ΔF) as a function of external Na^+ concentration, [Na^+]. Data were obtained from the same oocyte. The ordinate is expressed in arbitrary units (au) and corresponds to a change of fluorescence (ΔF) over baseline where Na^+ was replaced by choline (F_{total}). Scale: 1 au represents a $\Delta F/F_{total}$ of ~1%. The ΔF vs [Na^+] curves are sigmoidal and were drawn according to eq 1, $\Delta F = (\Delta F_{max}\text{-}[Na^+]^n)/\{[Na^+]^n + (K_{0.5})^n\}$, where ΔF_{max} is the maximal fluorescence for saturating [Na^+], $K_{0.5}$ is the half-maximal concentration, and n is the Hill coefficient. At −30 mV, $\Delta F_{max} = 7.4 \pm 1$ au, $K_{0.5} = 91 \pm 14$ mM, and $n = 2.0 \pm 0.2$. At −50 mV, $\Delta F_{max} = 7.5 \pm 1$ au, $K_{0.5} = 58 \pm 8$ mM, and $n = 1.9 \pm 0.2$. At −90 mV, $\Delta F_{max} = 8.2 \pm 0.8$ au, $K_{0.5} = 49 \pm 5$ mM, and $n = 1.8 \pm 0.2$. $K_{0.5}$ for Na^+ decreased further with greater hyperpolarizing potentials: for example, at $V_m = -150$ mV, in two experiments, $K_{0.5}$ was 25 and 35 mM (not shown).

held constant, at −30, −50, and −90 mV. At each holding potential, increasing the external Na^+ concentration increased rhodamine fluorescence. Likewise, at constant [Na^+], hyperpolarizing membrane potentials increased the fluorescence. The sigmoid ΔF versus [Na^+] relations were drawn according to eq 1. At all membrane potentials, the Hill coefficient was 2. The half-maximal concentration for Na^+ ($K_{0.5}$) was voltage dependent and decreased from 91 mM at −30 mV to 49 mM at −90 mV and to 30 mM at −150 mV (not shown).

Voltage Dependence. The dependence of the changes in fluorescence on membrane voltage was studied by keeping the external Na^+ concentration constant while stepping the membrane voltage to different values. Figure 4A (top panel) shows the time course of the changes in fluorescence with [Na^+] at 100 mM. In the experiment, the membrane potential was held at −50 mV and then stepped to a series of test voltages from +90 to −190 mV for 75 ms before being returned to the holding potential. For both depolarizing and hyperpolarizing voltage pulses, the fluorescence signal reached a steady-state level within 75 ms, which was maintained until the membrane potential was returned to the holding value. From the holding potential, positive-going potentials decreased the fluorescence signal, whereas hyperpolarizing potentials increased the signal. Figure 4B shows the relationship between the change in fluorescence (ΔF) and the test voltage (V_m). The sigmoid curves were drawn according to the Boltzmann function (eq 2). The maximal change in fluorescence, ΔF_{max}, which is the difference (estimated) in fluorescence between the depolarizing and hyperpolarizing saturating limits, was largest at 100 mM Na^+ and decreased ~20% at 25 mM [Na^+]. $V_{0.5}$, the median of the Boltzmann distribution, or the voltage at 50% ΔF_{max}, shifted from −58 to −125 mV with a 4-fold decrease in [Na^+] (from 100 to 25 mM; Figure 4A, middle panel, and Figure 4B). We studied the dependence of $V_{0.5}$ on [Na^+] (determined from 25, 50, 75, and 100 mM Na^+) and obtained a shift (to more negative voltages) of 114 ± 15 mV/10-fold reduction in [Na^+]. The apparent valence of the voltage sensor (z) was 0.4 ± 0.02 and was independent of [Na^+]. A change in fluorescence with voltage jumps was also observed in Na^+-free solutions (by replacement with choline; Figure 4A, bottom panel). Within the voltage range studied (−190 and +90 mV), the ΔF vs V_m curve did not show any tendency toward saturation with the most negative membrane voltage applied, and so it was not possible to obtain estimates of z, $V_{0.5}$, and ΔF_{max}. Since H^+ can substitute for Na^+ in SGLT1 (*9*), we determined whether there were any contributions from H^+ to the fluorescence in Na^+-free medium. In three experiments, the change in fluorescence intensity vs voltage curves was identical in choline medium at pH 7.4 and 8.4 (data not shown), indicating that there was no contribution of H^+ to the fluorescence signal at pH 7.4.

Figure 4C shows a comparison of the charge vs voltage (Q vs V_m) and change in fluorescence intensity vs voltage (ΔF vs V_m) curves obtained from the same oocyte. In 100 mM NaCl, the Q vs V_m and the ΔF vs V_m curves were both sigmoidal, and fits of the curves to the Boltzmann relation (eq 2) yielded similar $V_{0.5}$'s (~−50 mV). However, the apparent valence of the movable charge (z) was 1.0 for charge movement and 0.4 for the fluorescence.

The relaxation time constants (τ) for the ON and the OFF responses of the charge movement and fluorescence change are shown in Figure 4D. In this experiment, the membrane potential was held at −50 mV. For the ON response, the time constant of the charge movement decreased with depolarizing membrane voltages, from 20 ms at −150 mV to 5 ms at +50 mV. This is similar to wild-type human SGLT1 (*10*). In contrast, the time constant for fluorescence change was independent of membrane voltage ($\tau \sim 9$ ms). In the OFF response, τ was 9−10 ms for both and was independent of membrane voltage.

Sugar Dependence. The fluorescence intensity of TMR6M-labeled Q457C was sensitive to sugars when Na^+ was in the external medium. Figure 5A shows an experiment where the membrane potential was maintained at −50 mV. The oocyte was initially bathed in NaCl buffer. When 100 mM mannitol was added to the NaCl buffer, there was no effect on fluorescence (data not shown). To examine the effect of other sugars, mannitol (100 mM) was included in the perfusing NaCl buffer and was replaced (equimolar) by various concentrations of αMDG. The fluorescence intensity increased with increasing αMDG concentrations, and the dependence of ΔF on [αMDG] is shown in Figure 5B. The relationship was hyperbolic with a $K_{0.5}$ for αMDG of 38 mM (at −50 mV). The fluorescence signal also increased on addition of D-glucose and D-galactose. However, the fluorescence versus concentration relations (ΔF vs [D-glucose] and ΔF vs [D-galactose]) for both sugars did not show saturation at the highest sugar concentration used (100 mM), indicating that the $K_{0.5}$ values are very high (≥200 mM).

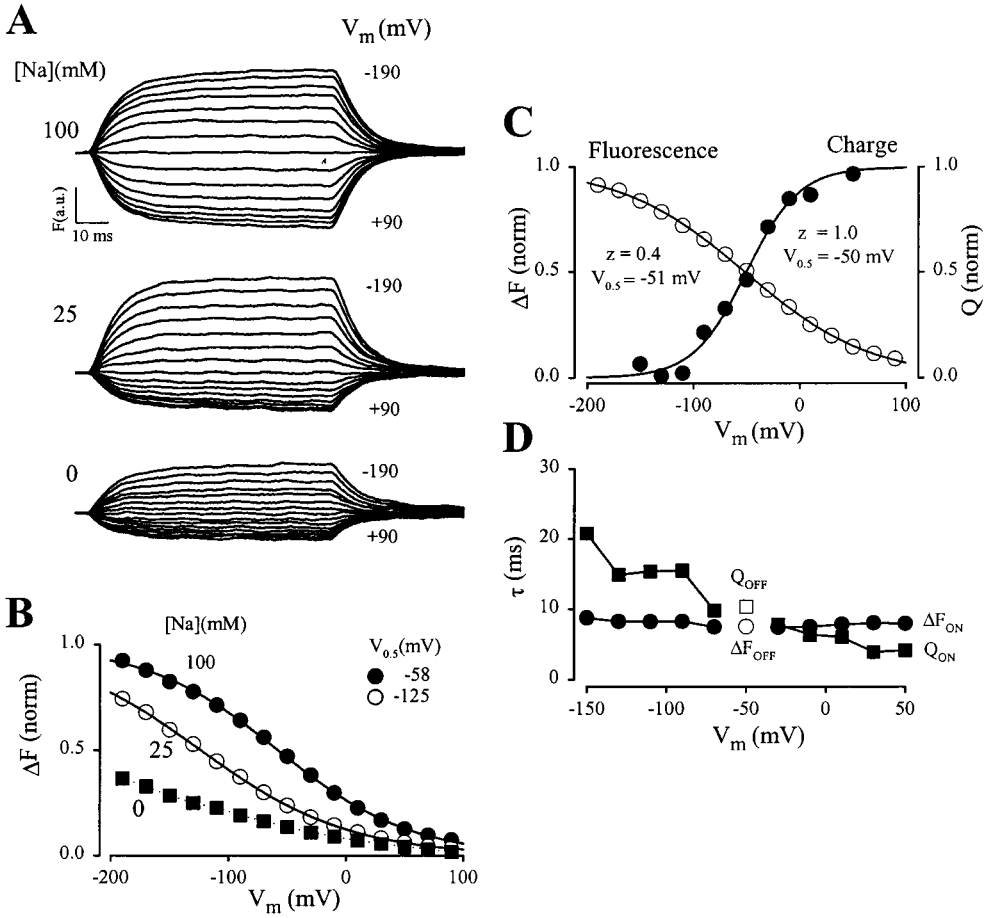

FIGURE 4: Changes in fluorescence with step jumps in membrane voltage. (A) Time course of the change in fluorescence with step jumps of the membrane voltage. V_h was −50 mV and then stepped (75 ms duration) from +90 to −190 mV with 20 mV increments. Scale: 1 au represents a $\Delta F/F_{total}$ of ∼1%. The experiments were performed with external solution containing 100 mM (top panel), 25 mM (middle panel), and 0 mM Na^+ (choline replacement, bottom panel). Data were obtained from a single oocyte, with 90% of the transporters labeled with TMR6M. A downward deflection of the traces indicates a decrease in fluorescence intensity. (B) Relationship between the change in fluorescence intensity (ΔF) and the test voltage V_m. ΔF is the difference in steady-state fluorescence between the test and holding potentials. The ΔF vs V relations for 100 and 25 mM [Na^+] were fitted to a Boltzmann function (eq 2): $(\Delta F - \Delta F_{hyp})/\Delta F_{max} = 1/[1 + \exp(z(V_m - V_{0.5})F/RT)]$, where $\Delta F_{max} = \Delta F_{dep} - \Delta F_{hyp}$; ΔF_{dep} and ΔF_{hyp} are the ΔF at depolarizing and hyperpolarizing limits; F is the Faraday; R, the gas constant; T, the absolute temperature; $V_{0.5}$, the membrane potential at 50% ΔF_{max}; and z, apparent valence of the charge sensor of the fluorophore. At 100 mM [Na^+], $z = 0.4 \pm 0.02$, and $V_{0.5} = -50 \pm 2$ mV. At 25 mM [Na^+], $z = 0.4 \pm 0.01$, and $V_{0.5} = -125 \pm 3$ mV. For comparison, the curves have been normalized to the maximal fluorescence change (ΔF_{max}) observed in 100 mM Na^+ and have also been shifted to align at the extrapolated depolarizing limit (see ref *6*). (C) Comparion of voltage dependence of charge movement (Q) and fluorescence. The bath solution was 100 mM NaCl buffer. Q vs V and ΔF vs V relations were fitted to the Boltzmann equation with $z = 1.0 \pm 0.2$ and $V_{0.5} = -50 \pm 4.5$ mV for the Q vs V relation, and $z = 0.4 \pm 0.02$ and $V_{0.5} = -51.5 \pm 1.7$ mV for the ΔF vs V relation. (D) Dependence of relaxation time constant (τ) for charge movement and fluorescence on membrane voltage. The external solution was the 100 mM NaCl buffer. Membrane voltage was held at −50 mV and then stepped (ON) to a series of test voltages (from +50 to −150 in 20 mV decrements) for 75 ms before returning to the holding value (OFF). The time course of the relaxations of the charge movement and fluorescence for the ON and OFF responses were fitted to monoexponential functions. The data for the OFF responses for charge off (Q_{OFF}) and fluorescence (ΔF_{OFF}) were independent of membrane voltage. The error bars are plotted for the OFF responses and represent SEM from 10 measurements; for both Q_{OFF} and ΔF_{OFF}, the error was less than the size of the symbol.

Changes of fluorescence with addition of sugar (100 mM αMDG) were not observed in the absence of Na^+ (choline replacement; data not shown).

The conformational state of the Q457C in the presence of Na^+ alone differed from that in Na^+ and sugar. Figure 6A shows the changes in fluorescence when the membrane voltage was held at −50 mV and stepped to different values, under conditions when external solution contained Na^+ (top panel) and Na^+ and sugar [100 mM αMDG (bottom panel)]. There was a larger reduction of ΔF at depolarizing potentials in the presence of sugar than in its absence. The ΔF vs V_m relationship is shown in Figure 6B (filled symbols) with the sigmoidal curves normalized with respect to the ΔF_{max} in 100 mM alone and shifted to align at the extrapolated depolarizing limit. At depolarizing potentials, the decrease of fluorescence was greater than the corresponding decrease in the absence of sugar. In the presence of sugar, at hyperpolarizing potentials the fluorescence signal was near saturation. The maximal change in fluorescence (ΔF_{max}) in the presence of sugar (48 ± 2 au) was increased ≈20% compared to that in Na^+ alone (39 ± 1 au). $V_{0.5}$ was shifted to more depolarizing potentials, from −40 ± 1 to 2 ± 2 mV, but z was unaffected by the sugar (0.5 ± 0.03 to 0.5 ± 0.02).

DISCUSSION

hSGLT1 Q457R is a glucose−galactose−malabsorption (GGM) mutant protein in which sugar transport is blocked (*2, 11*). In the previous study it was found that when

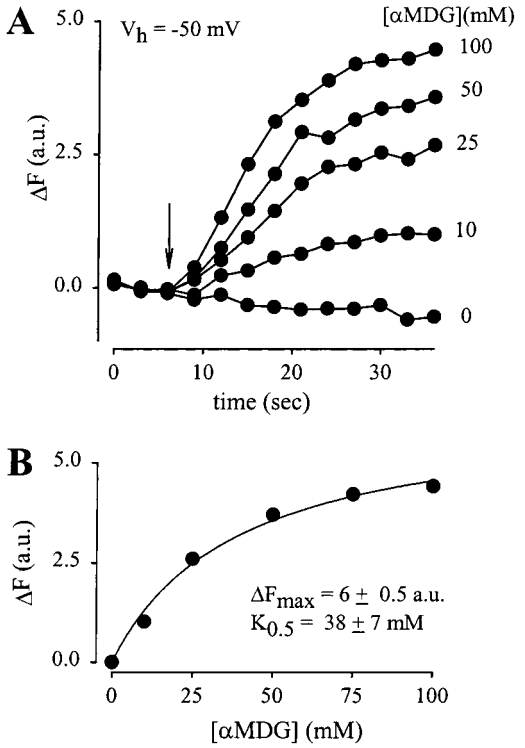

FIGURE 5: Dependence of fluorescence on sugar. (A) The dependency of fluorescence intensity on external sugar concentration was determined. The membrane potential was held at −50 mV, while the perfusing solution was changed from the NaCl buffer with 100 mM D-mannitol to the NaCl buffer containing different [αMDG] by equimolar replacement of D-mannitol. The arrow indicates the onset of the solution change. Addition of αMDG enhanced the fluorescence intensity in a concentration-dependent manner. (B) The sugar-induced increase in fluorescence (ΔF) was plotted as a function of external sugar concentration. The curve was drawn according to the equation $\Delta F = \Delta F_{max}[\alpha MDG]/([\alpha MDG] + K_{0.5})$, with $\Delta F_{max} = 6 \pm 0.5$ au and $K_{0.5} = 38 \pm 7$ mM.

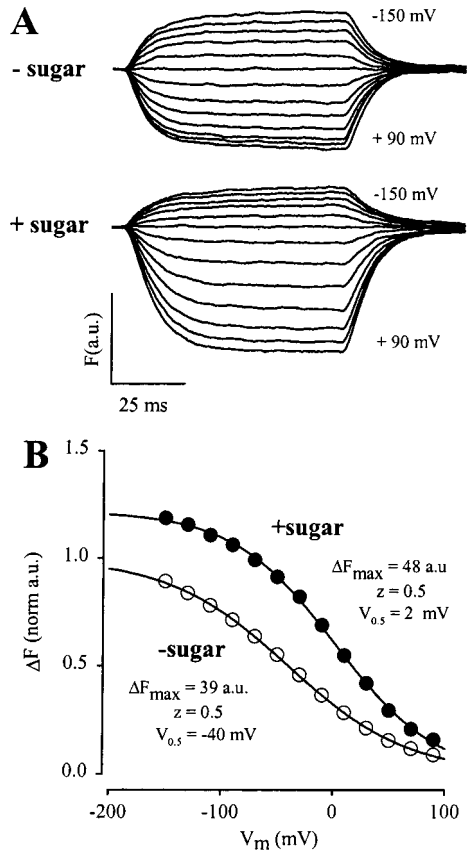

FIGURE 6: Effect of sugar on the fluorescence signal in voltage jumps experiments. (A) Time course of ΔF with step jumps of the membrane voltage in the absence (0 mM αMDG) and presence of 100 mM αMDG. V_h was −50 mV and was stepped from +90 to −190 mV with 20 mV increments in pulses of 75 ms duration. Bath NaCl concentration was 100 mM. Data were obtained from the same oocyte. (B) At each voltage, the difference in steady-state fluorescence (ΔF) between the test and holding voltage was plotted as function of the test voltage (V_m). The ΔF vs V curve was fitted to the Boltzmann function (see Figure 3). For comparison, the two curves have been normalized with respect to the ΔF_{max} (39 au) in 100 mM Na^+ alone and shifted so that the extrapolated limit at large depolarizing voltages is 0. In the absence of sugar, $\Delta F_{max} = 39 \pm 1$ au, $z = 0.5 \pm 0.02$, and $V_{0.5} = -40 \pm 1$ mV. When αMDG (100 mM) was added to the external solution, $\Delta F_{max} = 48 \pm 2$ au, $z = 0.5 \pm 0.03$, and $V_{0.5} = 2 \pm 2$ mV.

glutamine (at residue 457) is mutated to cysteine, Q457C regained full Na^+/sugar transport activity (*2*). However, sugar transport, as measured by tracer and current measurements, was blocked after exposure to TMR6M (*2*). The alkylation of Q457C by TMR6M (and other alkylating reagents on the cysteine at residue 457) could be detected as blockade of sugar transport, and this depended on the conformation of SGLT1; specifically it only took place in the presence of Na^+ at negative membrane voltages, i.e., in the Na^+-bound conformation of the transporter (*2*). The inhibitory action of TMR6M was blocked by external sugar and phlorizin. Blockade of sugar transport depended on the specific isomer of tetramethylrhodamine maleimide: the 6-isomer was more effective than the 5-isomer, since the 5-isomer did not label the transporter under the same labeling conditions (*2*). Even though TMR6M inhibited transport, sugar binding to the mutant protein Q457C still occurred; the half-maximal concentration ($K_{0.5}$) for αMDG is 12 ± 6 mM (*2*). Voltage jumps with TMR6M-labeled Q457C have shown that the changes in fluorescence closely followed the pre-steady-state charge movement and were blocked by phlorizin (1 mM). The correlation between charge movement and fluorescence indicates that charge movement is associated with protein conformational changes, and conformational states of the transporter (monitored by fluorescence) are altered by membrane voltage (*2*).

In the present study, the dependence of fluorescence (as a monitor of protein conformations) is extended to ligands. The fluorescence was sensitive only to substrates of SGLT1: Na^+ (and Li^+), but not TEA^+ or $NMDG^+$, increased fluorescence. The effect of Na^+ was saturable with a $K_{0.5}$ of 30 mM at −150 mV and a Hill coefficient of 2. The $K_{0.5}$ for Na^+ was voltage dependent. The sugar substrate also influenced fluorescence. αMDG increased fluorescence in Na^+ but not in choline. The increase was saturable with a $K_{0.5}$ of 38 ± 7 mM. The sugar specificity of the fluorescence was αMDG > D-glucose > D-galactose ≫ D-mannitol. The effects of membrane voltage on fluorescence were studied in the presence of Na^+ and sugar and in the absence of Na^+. Under Na^+-free conditions, there was a change in fluorescence with a change in membrane voltage, with a very negative $V_{0.5}$ (Figure 4B). A large negative $V_{0.5}$ in the absence of Na^+ has been predicted from pre-steady-state current analysis (*5*, *6*). In 100 mM Na^+, the $V_{0.5}$ for fluorescence is similar to charge movement (∼−50 mV). The apparent

valence z was 0.4 for fluorescence, compared to 1 for charge movement. The time constant of relaxation (τ) between −50 and +50 mV was in a range (5−10 ms) similar to that in the previous study (*2*). In contrast to the previous study, however, τ for fluorescence measured over a wider voltage range (−150 to +90 mV) was voltage independent for both the ON and OFF responses (Figure 4D). The difference in τ between fluorescence and charge movement indicates that charge movement is faster than fluorescence for depolarizing voltage jumps, and fluorescence is faster than charge movement for hyperpolarizing voltage steps (see below). When sugar was added to the external solution in the presence of Na^+, there was an increase in fluorescence: at close to saturating Na^+, there was a further increase in fluorescence on the addition of sugar at all membrane voltages, especially at −150 mV where 100 mM Na^+ is saturating. This suggests that there is an additional conformational change of the transporter on sugar binding (see below).

A Hill coefficient of 2 for Na^+ indicates that two Na^+ ions can bind to the cotransporter in the absence of sugar and that there is a high degree of cooperativity between the Na^+ sites. Binding of two Na^+ ions to SGLT1 in the absence of sugar agrees with the finding that the shift of the median voltage ($V_{0.5}$) of the pre-steady-state charge vs voltage (Q vs V) curve is 115 mV per 10-fold change in [Na^+] and is consistent with the involvement of two Na^+ ions in charge movement (*10*, *12*). The present data also provide evidence that binding of the Na^+ ions to the transporter is voltage dependent, with negative membrane potentials increasing the apparent affinity of the transporter for Na^+ (Figure 3).

Kinetic Model for Cotransport. We have previously proposed a six-state ordered alternating access kinetic model for Na^+/glucose cotransport that accounts both qualitatively and quantitatively for the observed kinetics of SGLT1 (*2*, *3*, *6*). The model assumes that the transporter has six kinetic states: the empty transporter C (states 1 and 6), the Na^+-bound CNa_2 (states 2 and 5), and the Na^+- and sugar-bound CNa_2S (states 3 and 4) in the external and internal membrane surfaces (Figure 7). In a transport cycle, on the external membrane surface the two Na^+ ions bind to the empty transporter before sugar ($1 \rightleftarrows 2$). After sugar binding ($2 \rightleftarrows 3$), there is a conformational change of the loaded complex ($3 \rightleftarrows 4$), resulting in substrate binding sites becoming accessible to the internal membrane surface, where the substrates are released. The empty substrate binding sites return to the external membrane surface via a conformational change: $6 \rightleftarrows 1$. The pre-steady-state currents are due to the conformational changes associated with Na^+ binding/dissociation ($1 \rightleftarrows 2$) and the conformational change of the empty transporter between the two membrane surfaces ($1 \rightleftarrows 6$). The model assumes that membrane voltage influences Na^+ binding/dissociation (≈30% of the membrane electric field) and the conformation of the empty transporter ($1 \rightleftarrows 6$) (≈70% of the membrane electric field) (*3*, *5*, *6*). As a consequence, there are two components of charge movement: 30% is due to Na^+ binding/dissociation and the remaining 70% to conformational change of the empty transporter (*3*, *5*, *6*). In the rhodamine-labeled hSGLT1 Q457C sugar transport is abolished; thus states 4 and 5 and the transitions between $3 \rightleftarrows 4 \rightleftarrows 5$ are eliminated. State 5 may be ignored in view of the low intracellular Na^+ concentrations in oocytes (≈5 mM; *13*) and the high $K_{0.5}$ for Na^+ in the intracellular membrane surface (70 mM; *14*).

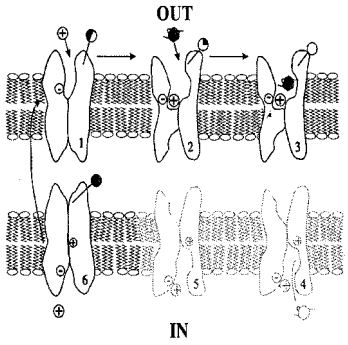

FIGURE 7: Cartoon showing the relationship between fluorescence and the six-state ordered kinetic model for Na^+/glucose cotransport. The transporter has six kinetic states consisting of the empty transporter C (states 1 and 6), the Na^+-bound CNa_2 (states 2 and 5), and the Na^+- and sugar-bound CNa_2S (states 3 and 4) in the external and internal membrane surfaces (modified from ref *2*). The empty transporter has a valence of −2. Two Na^+ ions bind to the transporter (forming an electroneutral complex CNa_2) before the sugar molecule. Membrane voltage influences the conformational change of the empty transporter ($1 \rightleftarrows 6$) between the external and internal membrane surfaces and the Na^+ binding/dissociation step ($1 \rightleftarrows 2$). The fluorophore (depicted by the circular bulb) is situated outside the membrane electric field. Fluorescence intensity is progressively increased (from dark to white bulb) as the transporter cycles through conformations $6 \rightarrow 1 \rightarrow 2 \rightarrow 3$. In the TMR6M-labeled Q457C sugar transport is abolished, thereby eliminating states 4 and 5 (faded symbols). The sugar binding reaction $2 \rightarrow 3$ involves an immediate $CNa_2S{:}2 \rightarrow CNa_2S \rightarrow 3$, where $CNa_2S \rightarrow 3$ represents the conformational change of the transporter after sugar binding.

Correlation of Fluorescence States with Kinetic States. From changes in fluorescence with varying Na^+ and sugar concentrations and membrane voltage we can now identify four conformational states of the transport cycle (Figure 7): the empty (states 1 and 6), the Na^+-bound (*2*), and the Na^+- and sugar-bound (state 3). In absence of Na^+, there is a voltage-dependent conformational change of the empty transporter ($1 \rightleftarrows 6$). Rhodamine fluorescence at residue 457 is increased in state 1 and decreased in state 6 (*2*, *4*−*6*). Addition of Na^+ to the external membrane surface increases the fluorescence in a dose-dependent manner with a Hill coefficient of 2, indicating that two Na^+ ions bind cooperatively to the transporter C (state 1) to form CNa_2 (state 2). The simplifying assumption in the model that the Na^+ binding reactions are written as a single step (*3*), which has been controversial (*15*, *16*), is justified by the finding of strong cooperativity between the Na^+ sites. One sugar molecule binds to the transporter in CNa_2 (state 2) to form CNa_2S (state 3). In the presence of sugar, the maximal rhodamine fluorescence ΔF_{max} is increased by 20% at every membrane voltage (Figure 6). This indicates that binding of sugar to the transporter in CNa_2 induces a conformational change, resulting in an increase in fluorescence. The transporter in the conformation CNa_2S (state 3) is the final product of sugar binding and probably represents a conformation that precedes the sugar translocation step. The sugar-bound CNa_2S (state 3) is distinct from the Na^+-bound CNa_2 (state 2) because of the fluorescence increase in the presence of sugar.

The observed fluorescence change (with step changes in membrane voltage) in the absence of Na^+ provides a novel insight into the distribution between two conformations of

the empty transporter, states 1 and 6: it is voltage dependent and follows the Boltzmann relation. $V_{0.5}$ is extrapolated to be more negative than −250 mV. The rate constants k_{16} (1 → 6) and k_{61} (6 → 1) for wild-type hSGLT1 have been estimated from analysis of pre-steady-state currents to be 600 s^{-1} and 25 s^{-1}, respectively, and at 0 mV membrane potential, the ratio $k_{16}/k_{61} = 600/25 = 24$ (*5*). For the TMR6M-labeled mutant Q457C, the present fluorescence result indicates that this ratio k_{16}/k_{61} is 1000 [the ratio of the probabilities of occupancy for the empty transporter with an apparent valence $z = 0.7$ (*4*−*6*) and a $V_{0.5}$ of −250 mV]. An underestimation of the ratio k_{16}/k_{61} may be the reason numerical simulations of the six-state kinetic model have failed to account for steady-state and pre-steady-state kinetic data on SGLT1 at low external Na^+ concentrations (*3*, *6*). The extremely negative $V_{0.5}$ (∼−250 mV) indicates that, without Na^+ in the external medium, high activation energy is required to shift the empty transporter from the internal to the external membrane surface (6 → 1). Simulation analysis of the sigmoidal activation curve (Figure 3) suggests that the binding of the first Na^+ ion to the transporter (in state 1) stabilizes that conformation, and the second Na^+ ion binds with an affinity much greater than the first.

Interpretation of Fluorescence Changes. Without information on the emission spectra of rhodamine fluorescence, we cannot assign the cause of the changes in fluorescence with substrates and membrane voltage—whether it's due to a Stokes shift or a quench of fluorescence (*17*). Starting from the conformation with lowest fluorescence intensity, state 6, as the transporter is sequentially put into the conformations 6 → 1 → 2 → 3 by Na^+ (and negative membrane voltage) and sugar, there is a progressive increase in fluorescence intensity (Figure 7). Interestingly, there is a parallel between the increase in rhodamine fluorescence with hyperpolarizing membrane voltages and the increase in rhodamine fluorescence in going from a polar to a hydrophobic environment (*18*): hyperpolarizing voltages shift the transporter to state 1, making the substrate binding sites accessible from the external membrane surface, and result in an increase in rhodamine fluorescence. Thus one possible interpretation is that the local environment of the fluorophore becomes progressively more hydrophobic as the transporter goes through the cycle: 6 → 1 → 2 → 3 (Figure 7). Two observations indicate that the above changes at residue 457 are localized to this part of the protein: (1) in the mutant hSGLT1 A166C the accessibility of alkylating reagents to the cysteine at residue 166 was independent of protein conformations (*19*), and (2) voltage-dependent fluorescence changes induced by ligands (Na^+ and sugar) were not observed in the mutants hSGLT1 A166C and I443C (both labeled with rhodamine methanethiosulfonate; unpublished observations).

The apparent valence of the movable charge (z) is 0.4 for fluorescence and 1.0 for charge movement. Pre-steady-state charge movement reflects global conformational changes of the transporter as the apparent valence of the movable charge ($z = z_1\delta_1 + z_2\delta_2 + ... + z_n\delta_n$) is the sum of the product of all movable charges (z_i) and the displacement (δ_i) of each charge in the membrane electric field, while the fluorescence signal reflects changes in the local environment of the fluorophore (around residue 457). For depolarizing voltages, the charge movement occurs at a faster rate than the fluorescence changes while for hyperpolarizing voltages, it occurs at a slower rate than the local conformational change monitored by fluorescence. The charge movement and fluorescence changes showed a different dependence on membrane voltage: the relaxation time constants (τ) for the fluorescence changes are independent of membrane voltage while τ for charge movement decreased with hyperpolarizing voltages. This differs from the previous study where $z = 1$ and the relaxation time constants for fluorescence and pre-steady-state current transients agree (*2*) and may be due to the increased signal to noise ratio of the fluorescence signal in the present experiments. The lack of voltage dependence for fluorescence relaxation is consistent with the finding that Q457C is not in the membrane electric field (*2*). The voltage dependence of the change in fluorescence suggests that motions of adjacent parts of the protein result in an environmental change around residue 457. The smaller value of z (0.4) indicates that the movements of these neighboring residues reflect the local contribution to the global conformational change and charge movement. The changes in local environment are related to the global protein conformation since the distribution of conformations, i.e., the dependence of $V_{0.5}$ on Na^+ concentration (∼100 mV/10-fold change in external [Na^+]) (*5*, *6*, *10*) is the same for charge movement and fluorescence (present study). The precise relationship between charge movement and fluorescence remains to be determined. The six-state kinetic model predicts a rapid component of charge movement (*6*), and in preliminary experiments with the cut-open preparation (*20*), we have observed rapid components of charge movement and rhodamine fluorescence (τ ∼100 μs).

In conclusion, using fluorescence as a probe of the local environment around the sugar translocation pathway of SGLT1, we interpret the changes of fluorescence as due to conformational changes of the transporter. Our results indicate that, under Na^+-free conditions, there is a voltage-dependent conformational change of the empty transporter (or ligand binding sites) between the external and internal membrane surface. In the absence of external Na^+, the empty ligand binding sites are situated exclusively on the internal membrane surface. On the external membrane surface, two Na^+ ions bind in a highly cooperatively manner to the transporter in the absence of sugar. After sugar is bound, the transporter undergoes a conformational change. Finally, the return of the empty ligand binding sites to the external membrane surface is greatly facilitated by binding to external Na^+: in the physiological voltage range (∼−50 mV), membrane voltage alone would exert a negligible effect on the return of the empty transporter to the external membrane surface.

ACKNOWLEDGMENT

We thank M. Lai-Bing and A. Johnson for the preparation and injection of oocytes, Drs. A. Cha and F. Bezanilla for valuable discussions on fluorescence experiments, and Drs. M. Panayotova-Heiermann and M. Quick for help with the illustrations.

REFERENCES

1. Mackenzie, B., Loo, D. D. F., and Wright, E. M. (1998) *J. Membr. Biol. 162*, 101−106.
2. Loo, D. D. F., Hirayama, B. A., Gallardo, E., Lam, J. T., Turk, E., and Wright, E. M. (1998) *Proc. Natl. Acad. Sci. U.S.A. 95*, 7789−7794.

3. Parent, L., Supplisson, S., Loo, D. D. F., and Wright, E. M. (1992) *J. Membr. Biol. 25*, 63−79.
4. Parent, L., Supplisson, S., Loo, D. D. F., and Wright, E. M. (1992) *J. Membr. Biol. 25*, 49−62.
5. Loo, D. D. F., Hazama, A., Supplisson, S., Turk, E., and Wright, E. M. (1993) *Proc. Natl. Acad. Sci. U.S.A. 90*, 5767−5771.
6. Hazama, A., Loo, D. D. F., and Wright, E. M. (1997) *J. Membr. Biol. 155*, 175−186.
7. Panayotova-Heiermann, M., Loo, D. D. F., Kong, C. T., Lever, J. E., and Wright, E. M. (1996) *J. Biol. Chem. 271*, 10029−10034.
8. Panayotova-Heiermann, M., Eskandari, S., Turk, E., Zampighi, G. A., and Wright, E. M. (1997) *J. Biol. Chem. 272*, 20324−20327.
9. Hirayama, B. A., Loo, D. D. F., and Wright, E. M. (1994) *J. Biol. Chem. 269*, 21407−21410.
10. Quick, M., Loo, D. D. F., and Wright, E. M. (2001) *J. Biol. Chem. 276*, 1728−1734.
11. Martin, M. G., Turk, E., Lostao, M. P., Kerner, C., and Wright, E. M. (1996) *Nat. Genet. 12*, 216−220.
12. Loo, D. D. F., Eskandari, S., Boorer, K. J., Sarkar, H. K., and Wright, E. M (2000) *J. Biol. Chem. 275*, 37414−37422.
13. Dascal, N. (1987) *Crit. Rev. Biochem. 22*, 317−387.
14. Sauer, G. A., Nagel, G., Koepsell, H., Bamberg, E., and Hartung, K. (2000) *FEBS Lett. 469*, 98−100.
15. Chen, X.-Z., Coady, M. J., Jala, F., Wallendorff, and Lapointe, J.-Y. (1997) *Biophys. J. 73*, 2503−2510.
16. Falk, S., Guay, A., Chenu, C., Patil, S. D., and Berteloot, A. (1998) *Biophys. J. 74*, 816−830.
17. Bezanilla, F. (2000) *Physiol. Rev. 80*, 555−592.
18. Mannuzzu, L. M., Moronne, M. M., and Isacoff, E. Y. (1996) *Science 271*, 213−216.
19. Meinild, A.-K., Loo, D. D. F., Hirayama, B. A., Gallardo, E., and Wright, E. M. (2001) *Biochemistry 40*, 11897−11904.
20. Cha, A., and Bezanilla, F. (1997) *Neuron 19*, 1127−1140.

BI011661R